10-21-2016

Block Ionomer Complexes Consisting of siRNA and *a*RAFT-Synthesized Hydrophilic-*Block*-Cationic Copolymers II: The Influence of Cationic Block Charge Density on Gene Suppression

Keith Hampton Parsons
University of Southern Mississippi, keith.parsons@usm.edu

Andrew Christopher Holley
University of Southern Mississippi, andrew.holley@eagles.usm.edu

Gabrielle A. Munn
University of Southern Mississippi

Alex S. Flynt
University of Southern Mississippi, alex.flynt@usm.edu

Charles L. McCormick
University of Southern Mississippi, Charles.McCormick@usm.edu

HHS Public Access

Author manuscript

Polym Chem. Author manuscript; available in PMC 2017 October 21.

Published in final edited form as:

Polym Chem. 2016 October 21; 7(39): 6044–6054. doi:10.1039/C6PY01048B.

Block ionomer complexes consisting of siRNA and *a*RAFT-synthesized hydrophilic-*block*-cationic copolymers II: The influence of cationic block charge density on gene suppression

Keith H. Parsons[a], **Andrew C. Holley**[a], **Gabrielle A. Munn**[a], **Alex S. Flynt**[b], and **Charles L. McCormick**[a,c]

[a]Department of Polymer Science and Engineering, The University of Southern, Mississippi, Hattiesburg, MS 39406, USA

[b]Department of Biological Sciences, The University of Southern Mississippi, Hattiesburg, MS 39406, USA

[c]Department of Chemistry and Biochemistry, The University of Southern Mississippi, Hattiesburg, MS 39406, USA

Abstract

Block ionomer complex (BIC)-siRNA interactions and effectiveness in cell transfection are reported. Aqueous RAFT polymerization was used to prepare a series of hydrophilic-*block*-cationic copolymers in which the cationic block statistically incorporates increasing amounts of neutral, hydrophilic monomer such that the number of cationic groups remains unchanged but the cationic charge density is diluted along the polymer backbone. Reduced charge density decreases the electrostatic binding strength between copolymers and siRNA with the goal of improving siRNA release after targeted cellular delivery. However, lower binding strength resulted in decreased transfection and RNA interference pathway activation, leading to reduced gene knockdown. Enzymatic siRNA degradation studies with BICs indicated lowered binding strength increases susceptibility to RNases, which is the likely cause for poor gene knockdown.

Introduction

RNA interference (RNAi) triggers post-transcriptional gene suppression via sequence-specific recognition and destruction of cellular transcripts.[1] “Gene knockdown” is achieved through delivery of synthetic small interfering RNA (siRNA), which can be designed to target the gene of interest,[2–5] making RNAi appealing for gene therapeutics. However, RNA delivery vehicles must overcome a number of barriers, including target specificity and vehicle cytotoxocity.[5]

Polymeric vectors can provide both enhanced stability and decreased immunogenic response relative to more traditional vectors (e.g. viral and lipid-based).[3] Of particular interest are polycationic polymers that electrostatically complex the negatively-charged RNA

[†]Electronic Supplementary Information (ESI) available: [details of any supplementary information available should be included here].

phosphodiester backbone to form interpolyelectrolyte complexes (IPECs).[6,7] Such IPECs are often characterized by the molar ratio of cationic functionalities (e.g. amines) to phosphodiester units, termed the nitrogen-to-phosphate ratio (N:P). Non-stoichiometric IPECs from cationic homopolymers have been extensively studied and provide enhanced protection from enzymatic degradation while maintaining complex hydrophilicity.[3,8] However, the excess charges required to maintain solubility result in adverse effects: negatively-charged complexes (N:P < 1) suffer from decreased transfection due to electrostatic repulsion at the negatively-charged cellular membrane, and positively-charged complexes (N:P > 1) result in increased cytotoxity and opsonization within the blood stream, leading to higher immune response.[6,9–11] Block copolymers consisting of a cationic block and a non-ionic, hydrophilic block can form stoichiometric, neutrally charged IPECs with RNAs while maintaining complex hydrophilicity. These so-called block ionomer complexes (BICs) exhibit both decreased cytotoxicity and enhanced stability,[7,12] and incorporation of cellular targeting moieties within their hydrophilic, corona-forming blocks results in cell-specific siRNA delivery.[8,13]

Our research group has maintained a strong interest in the rational design and synthesis of drug delivery systems utilizing aqueous RAFT (*a*RAFT) polymerization targeting controlled, tailored (co)polymers for stimuli-responsive micelles,[14–16] theranostics,[17] peptide mimics,[18] modular copolymers,[19,20] and vehicles for endosomal escape.[21] Our most recent efforts have focused on the development of siRNA-containing BICs for cell-specific delivery as well as determining the effect of *a*RAFT copolymer architecture on siRNA delivery efficacy. Previously, we demonstrated targeted cellular delivery and subsequent gene knockdown using BICs formed between siRNA and hydrophilic-*block*-cationic copolymers.[13] Furthermore, we observed a correlation between cationic block length and siRNA stabilization as well as gene knockdown efficacy: longer cationic block lengths resulted in increasingly enhanced siRNA stability as well as longer time periods required to achieve maximum gene knockdown *in vitro*.[22] We attributed delayed gene suppression to slow release of the siRNA from the complexes, presumably via macromolecular exchange. This correlates well with other groups' findings that enhanced complexation and stability in plasmid DNA (pDNA) delivery result in inefficient DNA release, indicating that intermediate binding and stability is desireable.[23–25] Such intermediacy is likely achievable via alteration of the cationic charge density. Indeed, IPECs formed from polymers with varying degrees of cationic quaternization yield higher pDNA transfection efficiency and expression at moderate charge densities as compared to linear polycations.[24,25] However, variable charge density has not been studied in BICs, specifically those containing siRNA.

In this study, we report the synthesis of a series of hydrophilic-*block*-cationic copolymers via *a*RAFT polymerization in which the cationic block statistically incorporates increasing amounts of neutral, hydrophilic monomer such that the number of cationic groups remains unchanged but the cationic charge density is diluted along the polymer backbone. These polymers were subsequently complexed with siRNA and siRNA analogs. To our knowledge, this is the first study directed toward elucidating the effect of cationic block charge density on BIC binding strength/stability and siRNA delivery. siRNA stability and BIC binding strength were evaluated utilizing solution differential scanning calorimetry (DSC) and potentiometric titration respectively, and cellular siRNA delivery experiments were

performed to correlate those results with gene knockdown efficacy. Herein, we demonstrate reduced siRNA stability, binding strength, and gene knockdown with decreasing cationic block charge density. We correlate these trends to reduced siRNA delivery and uptake within the RNAi pathway, which suggests greater siRNA vulnerability to enzymatic degradation. Indeed, we confirm higher rates of enzymatic hydrolysis with reduced cationic charge density by establishing RNase degradation kinetic profiles. We conclude that while reduced binding strength results in more rapid siRNA release via macromolecular exchange, such facile exchange increases the likelihood of degradation prior to activation of the RNAi pathway.

Results and Discussion

Synthesis of hydrophilic-*block*-cationic copolymers with varying cationic block charge density

Based upon our previous observation that decreasing cationic block length reduces the time required to achieve maximum gene knockdown,[22] we reasoned that reduced cationic block charge density should decrease BIC binding strength, facilitating the release of siRNA from the complexes via more rapid macromolecular exchange.

We therefore synthesized hydrophilic-*block*-cationic copolymers with varying cationic block charge density (Scheme 1). The first step was accomplished using *a*RAFT to prepare a statistical macroCTA consisting of an initial monomer feed ratio of 95 mol % N-(2-hydroxypropyl)methacrylamide (HPMA) and 5 mol % N-(3-aminopropyl)methacrylamide (APMA) in 1 M acetate buffer (pH = 4.5) at 70 °C using 4-cyano-4-[(ethylsulfanylthiocarbonyl)sulfanyl]pentanoic acid (CEP) as the CTA and 4,4'-azobiscyanovaleric acid (V-501) as the initiator. HPMA contributes non-ionic hydrophilicity to the copolymer, and is known to be non-immunogenic,[26] promoting greater biocompatibility. Incorporation of the primary amine functionality of APMA provides a convenient handle for the conjugation of the cellular-targeting moiety folic acid. ^{1}H NMR analysis revealed a final copolymer composition of 97 mol % HPMA and 3 mol % APMA, which closely matches the monomer feed ratio.

The resulting poly($HPMA_{226}$-*stat*-$APMA_7$) macroCTA was subsequently subjected to a series of chain extensions with both HPMA and N-[3-(dimethylamino)propyl]methacrylamide (DMAPMA), targeting DMAPMA monomer molar feeds, and thus charge densities, of 100% (**P100**), 75% (**P75**), 50% (**P50**), 25% (**P25**), and 0% (**P0**)‡. The tertiary amines of DMAPMA provide cationic sites under physiological conditions (pH = ~7.4) for complexation with the negatively-charged siRNA backbone. Additionally, the statistical incorporation of HPMA within the cationic block allows for increased spacing of the cationic groups, and thus lower charge density, along the polymer backbone while minimizing inter- and intramolecular hydrophobic interactions of the copolymers. ASEC-MALLS chromatograms for the macroCTA and the chain extensions are shown in Figure 1, and the relevant polymer characterization data are summarized in Table

‡Discussion of experiments relating to control polymer **P0** can be found in the ESI†.

1. Shifts to lower elution volume while maintaining low dispersities (Đ < 1.2) indicate successful chain extension, and ^{1}H NMR analysis revealed block compositions (block A: HPMA-*stat*-APMA; block B: HPMA-*stat*-DMAPMA) closely matching the monomer feed ratios. Cationic block charge densities are reported as molar percentages of DMAPMA within block B.

The post-polymerization modification of APMA units with folic acid, which our group has previously demonstrated to function well as a cell-specific targeting moiety,[13] was monitored via UV-Vis spectroscopy (ESI† Figure S2). Based on an average extinction coefficient for free folic acid at pH = 7.4, approximately 4 of 7 possible APMA units per polymer were successfully labelled. This extent of folic acid conjugation, combined with low APMA molar content, resulted in hydrophilic-*block*-cationic copolymers capable of electrostatically complexing with oligonucleotides through the DMAPMA tertiary amines of cationic block B, while the hydrophilic, cellular-targeting block A maintains BIC solubility. Thus, oligonucleotide complexation with these well-defined hydrophilic-*block*-cationic copolymers with varying charge density allows for correlation of cationic block charge density to BIC complexation strength and *in vitro* gene knockdown.

Hydrophilic-*block*-cationic copolymers with varying charge density form stable, neutrally-charged complexes

Having successfully synthesized a series of hydrophilic-*block*-cationic copolymers with varying cationic block charge density, we used dynamic light scattering (DLS) and ζ-potential measurements to confirm their ability to complex siRNA while maintaining charge neutrality at N:P = 1. Table 2 presents the hydrodynamic radius (R_h) and ζ-potential of each copolymer-siRNA complex. The siRNA-containing BICs exhibited an average R_h of 9.6 nm, a value consistent with previously reported complexes of similar cationic content.[13] Copolymer solutions free of siRNA did not exhibit any particles visible by DLS (data not shown), indicating that the observed hydrodynamic radii indeed result from complex formation rather than copolymer aggregation. The near-zero ζ-potential values confirm complex charge neutrality, targeted for preventing cytotoxicity. The amount of polymer-complexed siRNA was quantified using the Agilent Bioanalyzer platform (electropherograms in ESI† Figure S6), and copolymers **P25-P100** complexed approximately 76% of available siRNA, which is comparable to our previous report.[27]

Reduced cationic block charge density decreases oligonucleotide stabilization

Relative oligonucleotide stability can be determined by elucidating the melting temperature (T_m), i.e. the temperature at which the double-stranded duplex separates into its single-stranded components. An increase in T_m, which is manifested as an endotherm maximum in the DSC thermogram, is indicative of increased duplex stability.[28]

Previous work in our laboratories used dsDNA as an analog to siRNA in order to ascertain the effect of cationic block length of the copolymer on oligonucleotide stability.[22] In the present study, we used samples **P0-P100** to prepare BICs with dsDNA, and the respective DSC thermograms are shown in Figure 2. Complexation results in increased T_m over that of free dsDNA (T_m = 54.4 °C).[22] Generally, T_m decreases with decreasing cationic block

charge density (**P75**, 83.3 °C > **P50**, 81.3 °C > **P25**, 75.0 °C). Although **P100** has a continuous (i.e. no neutral comonomer) cationic block, its actual number of charges (14 DMAPMA units) is lower than for polymers **P25-P75** (~20 DMAPMA units), resulting in a T_m = 81.0 °C. However, BICs formed with previously reported ($HPMA_{171}$-*stat*-$APMA_{13}$)-*block*-$DMAPMA_{27}$ (**P2**), which has a longer continuous cationic block, exhibit a dsDNA T_m value of 88.4 °C.[22] Therefore, we may conclude that the enhanced oligonucleotide stability afforded by complexation decreases as cationic block charge density decreases.

Reduced cationic block charge density reduces complex binding strength

Having confirmed that reduced charge density diminishes the oligonucleotide-stabilizing effect of complexation, we next sought to demonstrate that it similarly reduces BIC binding strength as characterized by the free energy of complex formation. The cationic nature of weak polyelectrolytes, such as those containing DMAPMA, is due to the pH-dependent protonation of the amine functionalities and thus can be monitored via potentiometric acid-base titration. From the potentiometric titrations of a polyelectrolyte and its corresponding IPEC, one can obtain the degrees of protonation (α, fraction of protonated amines) and complexation (θ, fraction of ionic complex pairs out of total possible pairs) respectively. Kabanov and co-workers[7] have demonstrated that for IPECs consisting of a weak polyelectrolyte (e.g. PDMAPMA) and a strong polyelectrolyte (e.g. siRNA), all of the protonated units of the weak polycation will form ionic pairs with a strong polyanion functionality, i.e. $\alpha = \theta$. Due to the cooperativity of IPEC formation, a shift ($\Delta pH(\alpha)$) occurs in the θ vs. pH curve of an IPEC relative to the α vs. pH curve of the corresponding free polycation (Figure 3A). The free energy of complex formation (ΔG_{total}) as a function of α, where $\alpha = \alpha_1$ ($= \theta_1$), is given by the following:[7]

$$\Delta G_{\text{total}} = -2.303\text{RT}\int_0^{\alpha_1} \Delta\text{pH}(\alpha)\,d\alpha$$

Evaluation of the binding strength of oligonucleotide-containing BICs by potentiometric titration is complicated by the pH-dependent protonation of DNA and RNA bases. Thus, in this study we have adopted an approach similar to that of Lee et al.[29] who used polystyrene sulfonate (PSS) as a strong polyanion analog that does not affect the titration curve over the pH range investigated. We selected PSS with low molecular weight (M_n = 16 kDa, DP ≈ 69) such that the number of anionic charges is similar to that of duplex siRNA (59 nucleotides).

Figure 3 depicts the α- and θ vs. pH curves for **P0-P100** and lists the free energies of complexation for copolymer-PSS BICs. In general, the magnitude of free energy decreases with decreasing cationic block charge density (**P75**, −3.28 kJ/mol; **P50**, −2.42 kJ/mol; **P25**, −1.35 kJ/mol). Consistent with the DSC experiments in the previous section, despite being a continuous cationic block, the fewer number of charges in **P100** relative to **P25-P75** results in a lower binding strength with a ΔG_{total} value of −2.61 kJ/mol. However, titration of ($HPMA_{171}$-*stat*-$APMA_{13}$)-*block*-$DMAPMA_{27}$ (**P2**)[22] with a longer continuous cationic block length yields a ΔG_{total} value of −4.4 kJ/mol. Thus, we may conclude that binding strength decreases with reduced cationic charge density.

Reduced charge density diminishes gene knockdown efficacy

Based on the trends of decreasing oligonucleotide stabilization and BIC binding strength with decreasing cationic block charge density, one would expect that decreased charge density would lead to greater bioavailability of the siRNA within cells via more rapid release and, therefore, enhanced gene knockdown. However, experimental results were opposite of this expectation. Figure 4A depicts the relative survivin mRNA levels 24 hours after treatment with copolymer-siRNA BICs. **P100** and **P75** copolymers resulted in 2- and 3-fold mRNA expression, respectively, relative to the Lipofectamine positive control. However, polymers with charge density less than 75% exhibited no decrease in survivin mRNA levels relative to the untreated negative control. Although diminished gene knockdown with reduced charge density is the opposite of the expected trend, these results are likely the result of more rapid macromolecular exchange due to reduced binding strength: rapid exchange with extra- and intracellular proteins results in reduced cellular delivery of siRNA and increased susceptibility to degradation by RNases (*vide infra*).

Cellular delivery and RNAi pathway activation decrease with reduced cationic block charge density

To determine the relative cellular loading of siRNA by each polymer, cells were treated with copolymer-(fluorescently-labelled siRNA) BICs and were subsequently imaged via confocal fluorescence microscopy (images in ESI† Figure S5). The corrected total fluorescence (CTF) of representative areas for each treated cell culture is depicted in Figure 4B, and decreasing cellular siRNA content was observed with decreasing cationic block charge density. Furthermore, statistical analysis of CTF revealed a significant decrease in siRNA content between **P75** and **P50**, which corresponds well to lack of gene knockdown for copolymers with charge density < 75%. Because siRNA release must result from a macromolecular exchange reaction rather than spontaneous dissociation,[7] the decreased cellular delivery must be the result of exchange reactions with biomacromolecules in the extracellular media. However, **P50** and **P25** successfully delivered moderate amounts of siRNA, yet no gene knockdown was observed, suggesting reduced siRNA participation in the RNAi pathway.

Quantification of protein-bound siRNA within the cells serves as an indication of the level of RNAi activity. Because the threshold in cationic block charge density required for successful gene knockdown lies between **P75** and **P50**, these copolymers were used to deliver radio-labelled siRNA, and the treated cells were subjected to cellular fractionation via sucrose density gradients. The fractions were then subjected to PAGE, followed by electroblotting to quantify the relative amounts of radio-labelled siRNA in each, depicted in Figure 4C. Higher fraction numbers correspond to increased gradient density; therefore, farther migration of siRNA into the heavier fractions is indicative of siRNA-protein complexes (i.e. siRNA entry into the RNAi pathway). siRNA levels have been normalized to fraction 1 (i.e. protein-free siRNA) for each cell culture. **P75** complexes resulted in a greater amount of protein-complexed siRNA relative to its protein-free siRNA than did **P50**, indicating that, in addition to increased cellular siRNA concentration, **P75** complexes resulted in a greater percentage of that siRNA participating in RNAi. Therefore, as cationic block charge density decreases, less siRNA is trafficked into the cells, and even less RNAi activation is achieved.

When taken in conjunction, the fluorescence microscopy and cell fractionation results suggest that instead of increasing siRNA bioavailability, decreasing cationic block charge density leaves the siRNA more vulnerable to enzymatic degradation by RNases within the cell culture media and within the cells themselves. Reineke and coworkers[30] reported similar results utilizing hydrophilic-*stat*-cationic and hydrophilic-*block*-cationic copolymers to deliver luciferase-expressing plasmid DNA (pDNA): statistical copolymerization of their tertiary amine-containing monomer resulted in decreased luciferase expression relative to the block copolymer. The authors suggested that statistical copolymerization may have resulted in more rapid complex dissociation and thus inefficient trafficking of the pDNA to the nucleus. Our demonstration of decreased BIC binding strength with lower charge density, along with diminishing siRNA delivery and RNAi activation, corroborates their conclusion: weaker binding likely results in more rapid macromolecular exchange with cellular proteins like RNases.

Enzymatic degradation rates increase as cationic block charge density decreases

Although siRNA degradation within cells cannot be directly observed, circular dichroism (CD) spectroscopy can be used to monitor the degradation kinetics of siRNA by RNases *in vitro*. The characteristic CD spectrum peaks of siRNA result from its secondary structure,[31] and thus we monitored the molar ellipticity at 212 nm ($[\theta]_{212}$) as the siRNA was hydrolyzed along its phosphodiester backbone by Riboshredder RNase blend (Figure 5A). Figure 5B depicts normalized $[\theta]_{212}$ of siRNA and copolymer-siRNA complexes as a function of time. Based upon the gene knockdown, cellular loading, and cell fractionation experiments, we expected to see an increase in the rate of degradation with decreasing cationic block charge density. Indeed the decay rate of $[\theta]_{212}$ increases from **P100** to **P0**, indicating that decreased charge density does result in decreased protection from enzymatic degradation. This notion is in good agreement with the decreased oligonucleotide stabilization and binding strength, determined via solution DSC and potentiometric titration respectively, as a function of decreasing charge density.

Conclusions

The *a*RAFT polymerization of hydrophilic-*block*-cationic copolymers with varying cationic block charge densities and their subsequent complexation with siRNA and siRNA analogs has been demonstrated. Reduced charge density in these BICs resulted in lower oligonucleotide stabilization and binding strength, characteristics that predict more rapid siRNA release and thus enhanced gene suppression. However, decreased cellular transfection and RNAi activation, which resulted in decreased gene knockdown, indicate that decreased binding strength afforded by reduced charge density promotes greater susceptibility to enzymatic degradation. Indeed the higher rate of *in vitro* RNase degradation with decreasing charge density supports this notion. Components of the RNAi pathway likely have a higher affinity for siRNA than do other RNA-binding proteins (e.g. RNases). Thus, they likely are able to extricate siRNAs from higher charge density copolymers, whereas less specific RNases cannot.

These results indicate that for hydrophilic-*block*-cationic copolymers with relatively few charges (i.e. ~20 DMAPMA units), siRNA delivery is most effective utilizing a fully charged cationic block without non-ionic comonomer. However, it is worth noting that decreasing cationic block charge density diminishes copolymer cytotoxicity (ESI† Figure S6). Thus, application of variable charge density to block copolymers with a greater number of DMAPMA units should improve polymer biocompatibility while providing sufficient number of cations to maintain siRNA protection. The effect of cationic block charge density in copolymers with greater cationic content is the subject of ongoing investigation.

Experimental

Materials

All reagents were purchased from Sigma and used as received unless otherwise noted. 4,4'-Azobiscyanovaleric acid (V-501) was purchased from Wako and was recrystallized twice from methanol. Azobisisobutyronitrile (AIBN) was recrystallized from methanol. N-(3-aminopropyl)methacrylamide hydrochloride (APMA) was purchased from Polysciences. N-[3-(dimethylamino)propyl]methacrylamide (DMAPMA) and triethylamine (TEA) were distilled prior to use. 4-cyano-4-[(ethylsulfanylthiocarbonyl)sulfanyl]pentanoic acid (CEP),[32] di-N-hydroxysuccinimide-activated folic acid (diNHS-FA),[13] and N-(2-hydroxypropyl)methacrylamide (HPMA)[33] were synthesized according to literature procedures. Sodium polystyrene sulfonate (PSS) (Mn = 14.2 kDa, Đ = 1.13) was purchased from Scientific Polymer Products. HPLC purified oligonucleotides (siRNA against human survivin; unlabelled and AlexaFluor594-labeled, pre-diced siRNA; and oligomeric dsDNA) were purchased from Integrated DNA Technologies, Inc. The siRNA sequences targeting human survivin are as follows: Sense strand 5′-AGCCCUUUCUCAAGGACCACCGCAUCU-3′ and the antisense strand 3′-UUUCGGGAAAGAGUUCCUGGUGGCGUAGAGGA-5′. The pre-diced siRNA sequences are as follows: Sense strand 5'-GCUGGACUCCUUCAUCAACdTdT-3' and the antisense strand 3'-dTdTCGACCUGAGGAAGUAGUUG-5' ("dT" indicates deoxythiamine DNA base). The dsDNA sequences are as follows: Sense strand 5'-AGATGTGCAATTTTGCTACCGCATCT-3' and the antisense strand 5'-AGGAGATGCGGTAGCAAAAGTTGCACATCTTT-3'. Oligonucelotides (siRNA and dsDNA) were heated at 95 °C for 10 min and were allowed to slowly cool to room temperature prior to use. Concentrations of oligonucleotide (siRNA and dsDNA) are reported as duplex concentrations unless otherwise noted. Gibco® RPMI 1640 cell culture media (with and without folic acid) and fetal bovine serum (FBS) were purchased from Life Technologies Corporation. KB cells were purchased from ATCC. For reactions requiring nitrogen, ultrahigh purity nitrogen (purity ≥ 99.998%) was used. Spectra/Por® regenerated cellulose dialysis membranes (Spectrum Laboratories, Inc) with a molecular weight cut-off of 12–14 kDa were used for dialysis.

Polymer Synthesis

Synthesis of poly(HPMA-*stat*-APMA) macroCTA—The macro chain transfer agent (macroCTA) was prepared employing V-501 as the primary radical source and CEP as the chain transfer agent at 70 °C. HPMA (12.61 g, 95.1 mmol) and APMA (894 mg, 5.0 mmol)

were added to a 250 ml round-bottomed flask and dissolved in 1 M acetate buffer (pH = 4.5) with a final volume of 100 ml ($[M]_0$ = 1 M). The initial feed composition was 95 mol % HPMA and 5 mol % APMA. The round-bottomed flask was septum-sealed and purged with nitrogen for 1 hour prior to polymerization. The macroCTA was prepared with a $[M]_0$/[CTA] ratio = 400 while the [CTA]/[I] ratio was kept at 5, and the reaction was allowed to proceed for 5 h. The polymerization was quenched by rapid cooling in liquid nitrogen followed by exposure to air. The macroCTA was isolated by dialysis (pH = 3–4) at 4 °C and recovered by lyophilization.

Synthesis of poly[(HPMA-*stat*-APMA)-*block*-(HPMA-*stat*-DMAPMA)] copolymers (P100, P75, P50, P25, and P0)—The poly(HPMA-*stat*-APMA) macroCTA was chain extended with HPMA and/or DMAPMA using V-501 as the primary radical source at 70 °C. The macroCTA, HPMA, and DMAPMA were dissolved in acetate buffer to give a total $[M]_0$ = 1 M. The HPMA and DMAPMA initial feed compositions were adjusted to 100 mol % DMAPMA (**P100**); 75 mol % DMAPMA and 25 mol % HPMA (**P75**); 50 mol % DMAPMA and 50 mol % HPMA (**P50**); 25 mol % DMAPMA and 75 mol % HPMA (**P25**); and 100 mol % HPMA (**P0**). The round-bottomed flask was septum-sealed and subsequently purged with nitrogen for 1 h prior to polymerization. Block copolymers were prepared with $[M]_0$/[CTA] = 200 while [CTA]/[I] was kept at 5. Each polymerization was terminated at predetermined time intervals by rapid cooling in liquid nitrogen and subsequent exposure to air. The poly[(HPMA-*stat*-APMA)-*block*-(HPMA-*stat*-DMAPMA)] copolymers were purified by dialysis (pH = 3–4) at 4 °C and recovered by lyophilization.

Block copolymer end-groups were removed via a standard literature procedure.[34] A typical reaction is as follows: poly[($HPMA_{226}$-*stat*-$APMA_7$)-*block*-$DMAPMA_{14}$] (**P100**) (575 mg, 14.3 μmol) was added to a 25 ml round-bottomed flask and dissolved in 6 ml of DMF. AIBN (70.4 mg, 0.429 mmol) was then added to the flask resulting in an AIBN/copolymer ratio of 30:1. The solution was then septum-sealed, purged with nitrogen for 1 h, and allowed to react at 70 °C for 4 h. The resulting copolymer was precipitated from DMF into cold anhydrous diethyl ether three times.

Copolymer functionalization with folic acid

DiNHS-FA was prepared following a slightly modified literature prcedure.[13] Briefly, folic acid (1.00 g, 2.3 mmol), NHS (1.30 g, 11.3 mmol), DCC (4.68 g, 22.7 mmol), and DMAP (277.5 mg, 2.3 mmol) were dissolved in 15 ml DMSO and stirred in the dark at room temperature for 24 h. The dicyclohexylurea precipitate was filtered off and the resulting solution was used without further purification.

The aforementioned diNHS-FA solution was then used to label the primary amine moieties of the APMA units in the chain-terminated block copolymers. A typical reaction is as follows: 49.5 mg (1.23 μmol) **P100** was dissolved in 1 ml DMSO along with 5 μL TEA to serve as a catalyst. 1.53 ml of the diNHS-FA solution was added dropwise and the resulting solution was stirred in the dark at room temperature for 48 h. The reaction was quenched by the addition of excess ammonium hydroxide (100% by volume), and this reaction was carried out for 24 h. The resulting solution was then dialyzed against 0.6 M NaCl for 24 h,

followed by dialysis against DI water for 3 days. The polymer was recovered via lyophilization.

Formation of hydrophilic-*block*-cationic/oligonucleotide complexes

Preparation of copolymer-dsDNA complexes for solution differential scanning calorimetry—Poly[(HPMA-*stat*-APMA)-*block*-(HPMA-*stat*-DMAPMA)]-dsDNA complexes were prepared with N:P = 1 (i.e. neutral complexes). The dsDNA duplex concentration was maintained at 75 μM for all complexes. A typical preparation is as follows: 177 μL of a 1.785 mM poly[($HPMA_{226}$-*stat*-$APMA_7$)-*block*-$DMAPMA_{14}$] (**P100**) stock solution was added to 375 μL of a 200 μM dsDNA stock. The solution was diluted with 448 μL sodium cacadylate buffer, and the resulting dsDNA-copolymer complex solution was vortexed and equilibrated for 30 min. After equilibration, the solution was degassed for 30 min prior to DSC measurements. The dsDNA and polymer stock solutions were prepared in 10 mM sodium cacadylate buffer at pH 7.2.

Preparation of copolymer-siRNA complexes for gene suppression—Folic acid-labelled poly[(HPMA-*stat*-APMA)-*block*-(HPMA-*stat*-DMAPMA)]-siRNA complexes were prepared with N:P = 1, and the siRNA concentration was maintained at 100 nM. A typical preparation is as follows: 2.8 μL of a 71.43 μM **P100** stock solution was added to 3.3 μL of a 20 μM siRNA stock solution. The complex solution was gently mixed and equilibrated for 20 minutes prior to dilution with 214 μL folate- and serum-free RPMI, followed by gentile mixing. The siRNA and polymer stock solutions were prepared in 10 mM phosphate buffer (pH = 7.4).

Cell Culture

KB cells were maintained and proliferated in RPMI 1640 (with folic acid) supplemented with 10% FBS at 37 °C in 95% air humidified atmosphere and 5% CO_2.

Gene Suppression of Human Survivin

24 hours prior to treatment, the KB cell medium was replaced with folic acid-free RPMI 1640 supplemented with 10% FBS. Cells (200,000 cells/mL, 500 μL) were seeded in a 48 well plate (Corning Inc.). Cells were treated with 50 μL of a polymer-siRNA complex solution. Lipofectamine 2000 (Invitrogen) was used as the positive control, and the Lipofectamine-siRNA complexes were prepared according to manufacturer protocol. The final siRNA concentration delivered was maintained at 100 nM. After 24 hours, total RNA was extracted with TriZol (Invitrogen) following manufacturer protocol. Survivin transcript abundance was determined using RT-qPCR. First strand cDNA was synthesized with the Reverse Transcription Kit (Fermentas). Amplification and quantification was carried out with a 2X qPCR mix containing SYBR green (Fisher Scientific) and a BioRad CFX 96. The primer pairs for detecting the survivin gene were 5′-AGCCCTTTCTCAAGGACCAC and 5′-TCCTCTATGGGGTCGTCATC. PCR primers for β-Actin gene were 5′-CATGTACGTTGCTATCCAGGC and 5′-CTCCTTAATGTCACGCACGAT.

Fluorescence Microscopy

24 hours prior to treatment, the KB cell medium was replaced with folic acid-free RPMI 1640 supplemented with 10% FBS. Cells (200,000 cells/mL, 2 mL) were seeded on cover glasses in a 6 well plate (Corning Inc.). Cells were treated with 500 μL of a polymer-siRNA (siRNA tagged with AlexaFluor594) complex solution. Lipofectamine 2000 (Invitrogen) was used as the positive control, and the Lipofectamine-siRNA complexes were prepared according to manufacturer protocol. The final siRNA concentration delivered was maintained at 100 nM. After 24 hours, the cells were fixed with 4% formaldehyde and washed with PBS prior to imaging. The cells were then stained with 12 μL of 4',6-diamidino-2-phenylindole (DAPI) mounting medium. The cover glasses were then placed on precleaned microscope slides for analysis. Fluorescence cell images were taken using a Zeiss LSM 510 scanning confocal microscope and processed with manufacturer software. Multiple fields were examined for each sample to ensure uniform distribution of complexes throughout. Representative areas were selected in quadruplicate, the fluorescence intensities were determined in ImageJ, and the corrected total fluorescence (CTF) of each area was calculated according to the relation

$$\mathrm{CTF}=\mathrm{Integrated\ \ Density}-(\mathrm{area}\times\mathrm{background\ \ mean\ \ fluroescence}).$$

Statistical variance between samples was calculated via a one-way ANOVA with Tukey analysis in Minitab (version 17.1.0).

Cell Fractionation

Prior to cell treatment, the siRNA 5'-phosphate was substituted with ^{32}P-containing phosphate using polynucleotide Kinase (Fisher) and γ-^{32}P ATP (6000 Ci/mmol) as the source of isotope. The KB cell medium was replaced with folic acid-free RPMI 1640 supplemented with 10% FBS. Cells (200,000 cells/mL, 2 mL) were seeded in a 6 well plate (Corning Inc.). After 24 hours, cells were treated with 500 μL of a radio-labelled polymer-siRNA complex solution. Lipofectamine 2000 (Invitrogen) was used as the positive control, and the Lipofectamine-siRNA complexes were prepared according to manufacturer protocol. The final siRNA concentration delivered was maintained at 100 nM. After 24 hours, the cell media was removed, and the cells were lysed with 1 mL lysing buffer (150 mM HEPES, pH = 8.0; 0.25% Triton X; 10% glycerol).

Linear sucrose gradients (10%-50% w/w in 25 mM Tris-HCl (pH = 7.5), 25 mM NaCl, 5 mM $MgCl_2$) were prepared by carefully layering 400 μL of each sucrose solution in a Beckman 13 × 51 mm thickwall polycarbonate tube at 0 °C. Total cell lysates were carefully overlaid onto the gradients and centrifuged at 36,000 rpm for 2 hrs at 4 °C in a SW 55 Ti rotor. Gradient fractions were then collected in 300 μL increments, and total RNA was precipitated into 1 ml of isopropanol, employing 1 μL glycogen solution as a co-precipitant. After centrifugation, the supernatant was removed, and the precipitants were suspended in 2X RNA loading buffer from Ambion. RNA was separated on a 12% acrylamide gel containing 8 M urea, and visualized with ethidium bromide staining on a BioRad ChemiDoc MP. The gel was then electroblotted and crosslinked. The radio-labelled siRNA was imaged using a GE Healthcare Life Sciences Typhoon FLA-7000. The relative amount of siRNA

was quantified in bands corresponding to both free siRNA and that loaded in protein complexes using densitometry software ImageQuant.

Copolymer Cytotoxicity

The anti-proliferative activities of poly[(HPMA-*stat*-APMA)-*block*-(HPMA-*stat*-DMAPMA)] copolymers were determined following a standard literature procedure. 24 hours prior to treatment, the KB cell medium was replaced with folic acid-free RPMI 1640 supplemented with 10% FBS. Cells (200,000 cells/mL, 100 μL) were seeded in a 96 well plate (Corning Inc.). Cells were treated with 50 μL of a polymer stock solution at a polymer concentration equivalent to that used in the gene suppression studies. Cell proliferation was determined via a standard MTT assay (Vybrant MTT Cell Proliferation Assay Kit; Invitrogen). Cells were incubated for 48 h and 72 h before adding 10 μL of a 12 mM MTT reagent to each well. The cells were further incubated for an additional 4 h, followed by adding 100 μL of a SDS (10%)/HCl (0.01 M) solution to each well. The absorbance was then determined utilizing a Biotek Synergy2 MultiMode Microplate Reader. All studies were performed in triplicate.

Characterization

All polymers were characterized by aqueous size exclusion chromatography (ASEC) with an eluent of 1 wt % acetic acid and 0.1 M Na_2SO_4 (aq) at a flow rate of 0.25 ml/min at 25 °C, Eprogen Inc. CATSEC columns (100, 300, and 1000 Å), a Wyatt Optilab DSP interferometric refractometer (λ = 690 nm), and a Wyatt DAWN-DSP multi-angle laser light scattering (MALLS) detector (λ = 633 nm). Absolute molecular weights and molecular weight distributions were calculated using Wyatt Astra (version 4) software. dn/dc measurements for all (co)polymers were performed utilizing a Wyatt Optilab DSP interferometric refractometer (λ = 690 nm) at 25 °C and Wyatt DNDC (version 5.90.03) software. Polymer monomer conversions were calculated by comparing the area of the monomeric refractive index signal at t_0 to the area at t_f.

Copolymer compositions were determined using a Varian MercuryPLUS 300 MHz NMR spectrometer in D_2O utilizing a delay time of 5 s. ^1H NMR was used to determine copolymer compositions by integration of the relative intensities of the methyne proton resonances of HPMA at 3.75 ppm and the dimethyl proton resonances of DMAPMA at 2.75 ppm. The number of monomer units were calculated as $n = (mol\% \times M_{n,\,Exp})/MW_{monomer}$. Conjugation of folic acid to the block copolymers was verified via UV-Vis spectroscopy using a PerkinElmer Lambda 35 spectrophotometer utilizing an average extinction coefficient of 8000 $M^{-1}cm^{-1}$ for free folic acid in phosphate buffter (10 mM P_i, 100 mM NaCl, pH = 7.4). ^1H NMR was performed using a Varian MercuryPLUS 300 MHz spectrometer in DMSO-d_6 with a delay time of 5 s. The amount of conjugated folic acid was estimated by integration of the methyne proton resonance of HPMA at 3.75 ppm and the proton resonance of folic acid at 8.64 ppm (s, PtC_7H, 1 ^1H). These values were estimated by employing a Lorentzian/Gaussian line fit using MestReNova (version 6.0.2–5475).

Variable-angle dynamic light scattering (DLS) measurements of copolymer-siRNA complexes under aqueous conditions were performed using an incident light of 633 nm from

a Research Electro-Optics Model 31425 He-Ne laser operating at 35 mW. The angular dependence (60°-120° in 10° increments) of the autocorrelation function was determined with a Brookhaven Instruments BI-200SM goniometer with an Avalanche photodiode detector and TurboCorr autocorrelator. DLS measurements were carried out at a complex concentration (siRNA + block copolymer) of 1.0 mg/ml in phosphate buffer (10 mM P_i, pH = 7.4) at 25 °C. The mutual diffusion coefficients (D_m) were determined from the relation

$$\Gamma = D_m q^2$$

in which Γ and q^2 represent the decay rate of the autocorrelation function and the square of the scalar magnitude of the scattering vector respectively. The hydrodynamic radius (R_h) was then calculated from the Stokes-Einstein equation:

$$D_m \approx D_0 = (k_B T)/(6\pi\eta R_h)$$

in which η is the solution viscosity, k_B is Boltzmann's constant, and T is the temperature in K. Samples were vortexed to ensure homogeneity and equilibrated for 30 min at 25 °C prior to measurement. To remove dust, samples were passed through a 0.45 μm Millipore filter (PVDF) directly into the scattering cells. Measurements were performed in triplicate.

Zeta-potential measurements were carried out at a complex concentration of 1.0 mg/ml in phosphate buffer (10 mM P_i, pH = 7.4) using a Malvern Zetasizer Nano ZEN3600. Samples were vortexed to ensure homogeneity and equilibrated for 30 min at 25 °C prior to measurement. To remove dust, samples were centrifuged at 14,000 RPM for 10 min. Measurements were performed in triplicate.

Quantification of polymer-complexed siRNA was achieved using the Agilent 2100 Bioanalyzer platform with the Small RNA kit following manufacturer protocol. Samples were prepared with [siRNA] = 100 nM, N:P = 1 in RNase-free water. Samples were vortexed to ensure homogeneity and equilibrated for 30 min at 25 °C prior to measurement. The free siRNA concentration was determined from the area of the peak at ~39 s using the companion software. Percent complexed siRNA was calculated as 1 – [$siRNA_{39s,\ complex}$]/[$siRNA_{39s,\ control}$].

All calorimetric experiments were carried out using a Calorimetric Sciences Corporation Nano DSC-II solution differential scanning calorimeter (DSC). Sodium cacadylate buffer (10 mM, pH = 7.2) was used as the running buffer. dsDNA (analog for siRNA) concentration was maintained at 75 μM while copolymer concentrations were adjusted to maintain N:P = 1. CpCalc (Version 2.1, Calorimetric Sciences Corp.) was used to subtract buffer-buffer scans from buffer-sample scans.

Potentiometric titration experiments were carried out using a Metrohm 848 Titrino Plus autotitrator. Polymer samples were prepared in 5.0 ml of 18.2 MΩ diH_2O and concentrations were adjusted to maintain a total amine concentration (i.e. DMAPMA unit concentration) of 1 mM. The pH of the solution was adjusted to 2.0 via the addition of 1 N HCl, followed by autotitration to pH = 12.0 with 0.05 N NaOH at 25 °C. For polymer-polystyrene sulfonate

(PSS) complex solutions, polymer stock solutions were adjusted to pH = 2.0 with 1 N HCl before addition to PSS stock solutions to afford neutral complexes (i.e. [DMAPMA] = [SS]) followed by dilution to 5.0 ml (final DMAPMA unit concentration = 1 mM). The complex solutions were then autotitrated to pH = 12 with 0.05 N NaOH. The degree of protonation (α) and degree of complexation (θ) as a function of pH for each polymer or polymer-PSS complex solution was determined from the titration curves according to literature procedure.[29]

The kinetics of degradation of free and complexed siRNA with Riboshredder RNase blend (Epicentre) were obtained by monitoring time-dependent ellipticity at λ = 212 nm utilizing a Jasco J-815 circular dichroism spectropolarimeter. Samples (V = 200 μL) were prepared in phosphate buffer (10 mM P_i, pH = 7.4) with [siRNA] = 5.0 μM. For complex solutions, the copolymer concentrations were adjusted to maintain N:P = 1. Samples were placed in a 400 μL quartz cuvette (path length = 1 mm), and the initial spectra from λ = 200–320 nm were recorded with a scan rate of 50 nm/min, a 0.5 nm bandwidth, and a time constant of 2 s. The signal-to-noise was doubled for all spectra by averaging four scans. After establishing a baseline, 0.63 μL of Riboshredder stock solution (0.25 unit/μL diluted in 10 mM P_i, pH = 7.4) was added followed by inversion of the cuvette to promote mixing. The ellipticities at λ = 212 nm were then recorded over 20 min. with a 0.5 nm bandwidth and a time constant of 2 s.

Supplementary Material

Refer to Web version on PubMed Central for supplementary material.

Acknowledgments

The authors would like to thank Dr Reid Bishop, Dr Vijay Rangachari, and Dr Daniel Savin for the use of the solution differential scanning calorimeter, CD spectropolarimeter, and the DLS instruments, respectively. This work was funded through NSF EPSCoR EPS-0903727. This work was supported by the Mississippi INBRE, funded by an Institutional Development Award (IDeA) from the National Institute of General Medical Sciences of the National Institutes of Health under grant number P20GM103476.

Notes and References

1. Fire A, Xu S, Montgomery MK, Kostas SA, Driver SE, Mello CC. Nature. 1998; 391:806–811. [PubMed: 9486653]
2. Elbashir SM, Harborth J, Lendeckel W, Yalcin A, Weber K, Tuschl T. Nature. 2001; 411:494–498. [PubMed: 11373684]
3. Pack DW, Hoffman AS, Pun S, Stayton PS. Nat. Rev. Drug Discov. 2005; 4:581–593. [PubMed: 16052241]
4. Dorsett Y, Tuschl T. Nat. Rev. Drug Discov. 2004; 3:318–329. [PubMed: 15060527]
5. Sarisozen C, Salzano G, Torchilin VP. Biomol. Concepts. 2015; 6:321–341. [PubMed: 26609865]
6. Gebhart CL, Kabanov AV. J. Control. Release. 2001; 73:401–416. [PubMed: 11516515]
7. Kabanov V, Kabanov A. Adv. Drug Deliv. Rev. 1998; 30:49–60. [PubMed: 10837601]
8. Park TG, Jeong JH, Kim SW. Adv. Drug Deliv. Rev. 2006; 58:467–486. [PubMed: 16781003]
9. Fischer D, Li Y, Ahlemeyer B, Krieglstein J, Kissel T. Biomaterials. 2003; 24:1121–1131. [PubMed: 12527253]
10. Deshpande MC, Davies MC, Garnett MC, Williams PM, Armitage D, Bailey L, Vamvakaki M, Armes SP, Stolnik S. J. Control. Release. 2004; 97:143–156. [PubMed: 15147812]

11. Merdan T, Kunath K, Fischer D, Kopecek J, Kissel T. Pharm. Res. 2002; 19:140–146. [PubMed: 11883640]
12. Kamimura M, Kim JO, V Kabanov A, Bronich TK, Nagasaki Y. J. Control. Release. 2012; 160:486–494. [PubMed: 22546682]
13. York AW, Zhang Y, Holley AC, Guo Y, Huang F, McCormick CL. Biomacromolecules. 2009; 10:936–943. [PubMed: 19290625]
14. Smith AE, Xu X, Kirkland-York SE, Savin DA, McCormick CL. Macromolecules. 2010; 43:1210–1217.
15. Smith AE, Xu X, Savin DA, McCormick CL. Polym. Chem. 2010; 1:628–630.
16. Flores JD, Xu X, Treat NJ, McCormick CL. Macromolecules. 2009; 42:4941–4945.
17. Kirkland-York S, Zhang Y, Smith AE, York AW, Huang F, McCormick CL. Biomacromolecules. 2010; 11:1052–1059. [PubMed: 20337403]
18. Treat NJ, Smith D, Teng C, Flores JD, Abel BA, York AW, Huang F, McCormick CL. ACS Macro Lett. 2012; 1:100–104. [PubMed: 22639734]
19. Flores JD, Treat NJ, York AW, McCormick CL. Polym. Chem. 2011; 2:1976.
20. Flores JD, Shin J, Hoyle CE, McCormick CL. Polym. Chem. 2010; 1:213.
21. Holley AC, Ray JG, Wan W, Savin DA, Mccormick CL. Biomacromolecules. 2013; 14:3793–3799. [PubMed: 24044682]
22. Holley AC, Parsons KH, Wan W, Lyons DF, Bishop GR, Correia JJ, Huang F, McCormick CL. Polym. Chem. 2014; 5:6967–6976.
23. MacLaughlin FC, Mumper RJ, Wang J, Tagliaferri JM, Gill I, Hinchcliffe M, Rolland AP. J. Control. Release. 1998; 56:259–272. [PubMed: 9801449]
24. Song Y, Wang H, Zeng X, Sun Y, Zhang X, Zhou J, Zhang L. Bioconjug. Chem. 2010; 21:1271–1279. [PubMed: 20521783]
25. Allen MH, Green MD, Getaneh HK, Miller KM, Long TE. Biomacromolecules. 2011; 12:2243–2250. [PubMed: 21557603]
26. Kopecek J. Biomaterials. 1984; 5:19–25. [PubMed: 6375745]
27. Scales CW, Huang F, Li N, Vasilieva Ya, Ray J, Convertine AJ, McCormick CL. Macromolecules. 2006; 39:6871–6881.
28. Sturtevant J. Annu. Rev. Phys. Chem. 1987; 38:463–488.
29. Lee H, Son SH, Sharma R, Won Y-Y. J. Phys. Chem. B. 2011; 115:844–860. [PubMed: 21210675]
30. Sprouse D, Reineke TM. Biomacromolecules. 2014; 15:2616–2628. [PubMed: 24901035]
31. Bishop GR, Chaires JB. Curr. Protoc. Nucleic Acid Chem. 2003; Chapter 7 Unit 7.11.
32. Convertine AJ, Benoit DSW, Duvall CL, Hoffman AS, Stayton PS. J. Control. Release. 2009; 133:221–229. [PubMed: 18973780]
33. Kopeček J, Bažilová H. Eur. Polym. J. 1973; 9:7–14.
34. Perrier S, Takolpuckdee P, Mars CA. Macromolecules. 2005; 38:2033–2036.

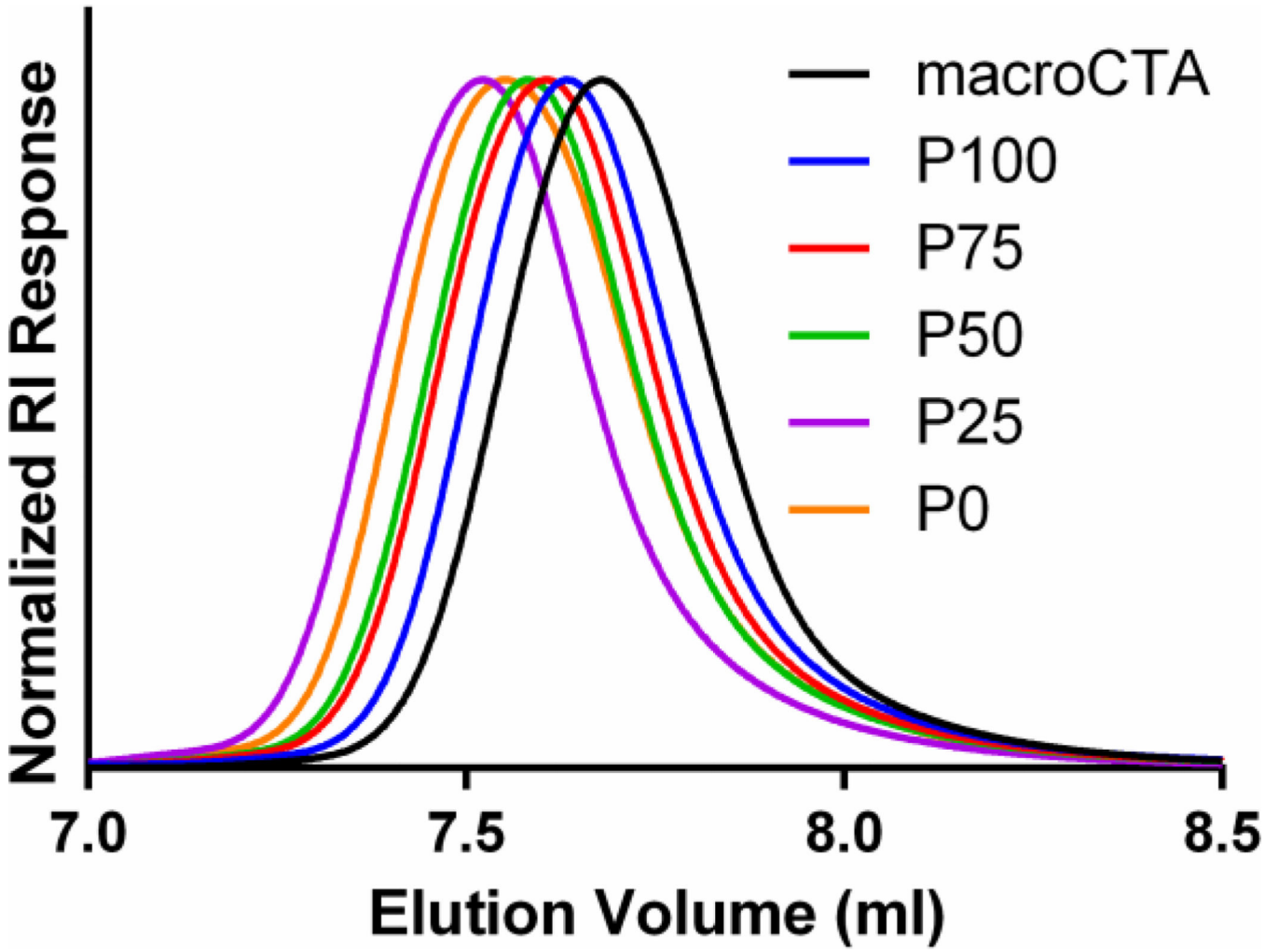

Figure 1.
ASEC-MALLS of poly(HPMA-*stat*-APMA) macroCTA and subsequent chain extensions with DMAPMA and HPMA (**P100-P0**)

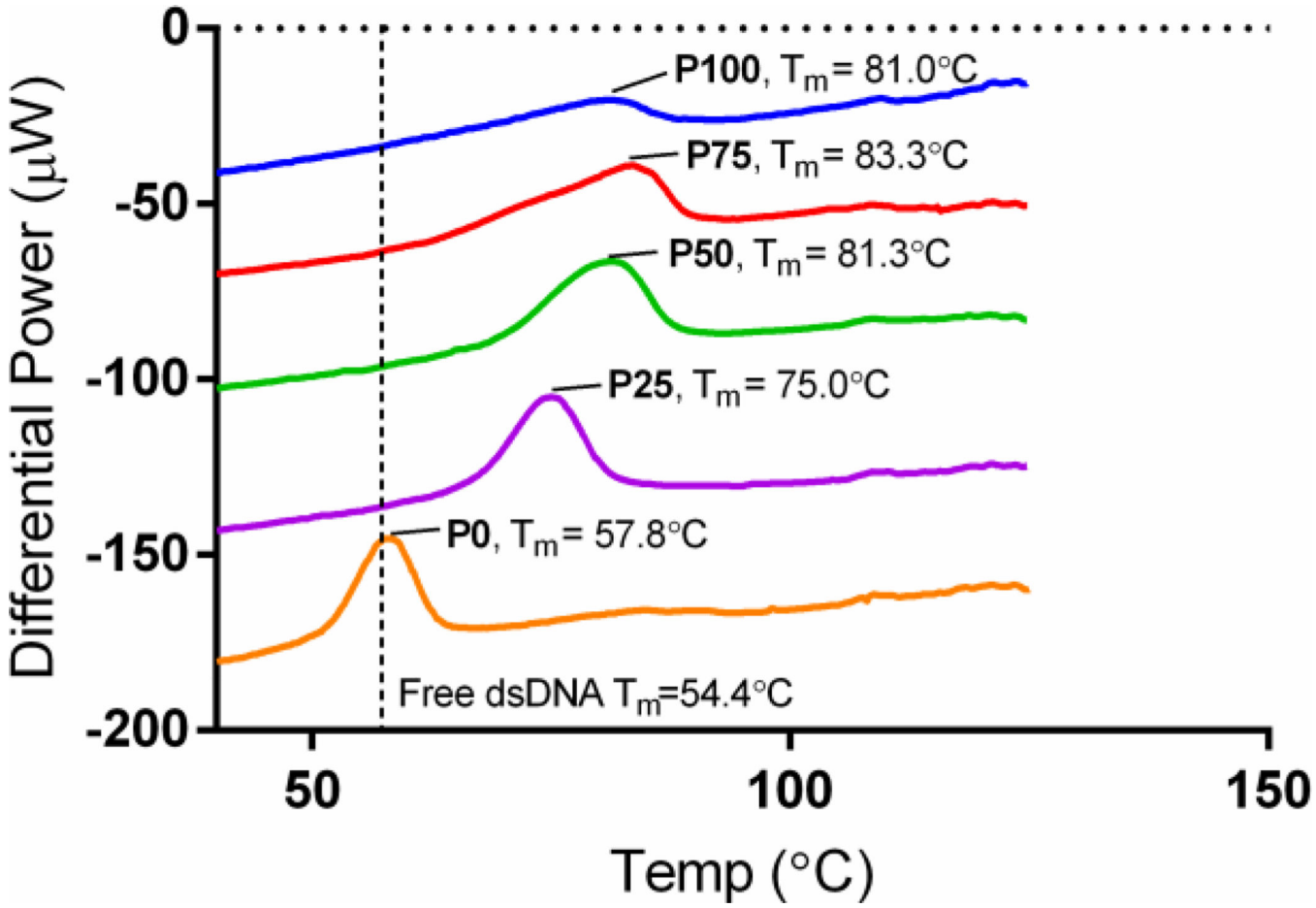

Figure 2.
Differential power thermograms for copolymer-dsDNA complexes. Samples shifted along Y-axis for clarity.

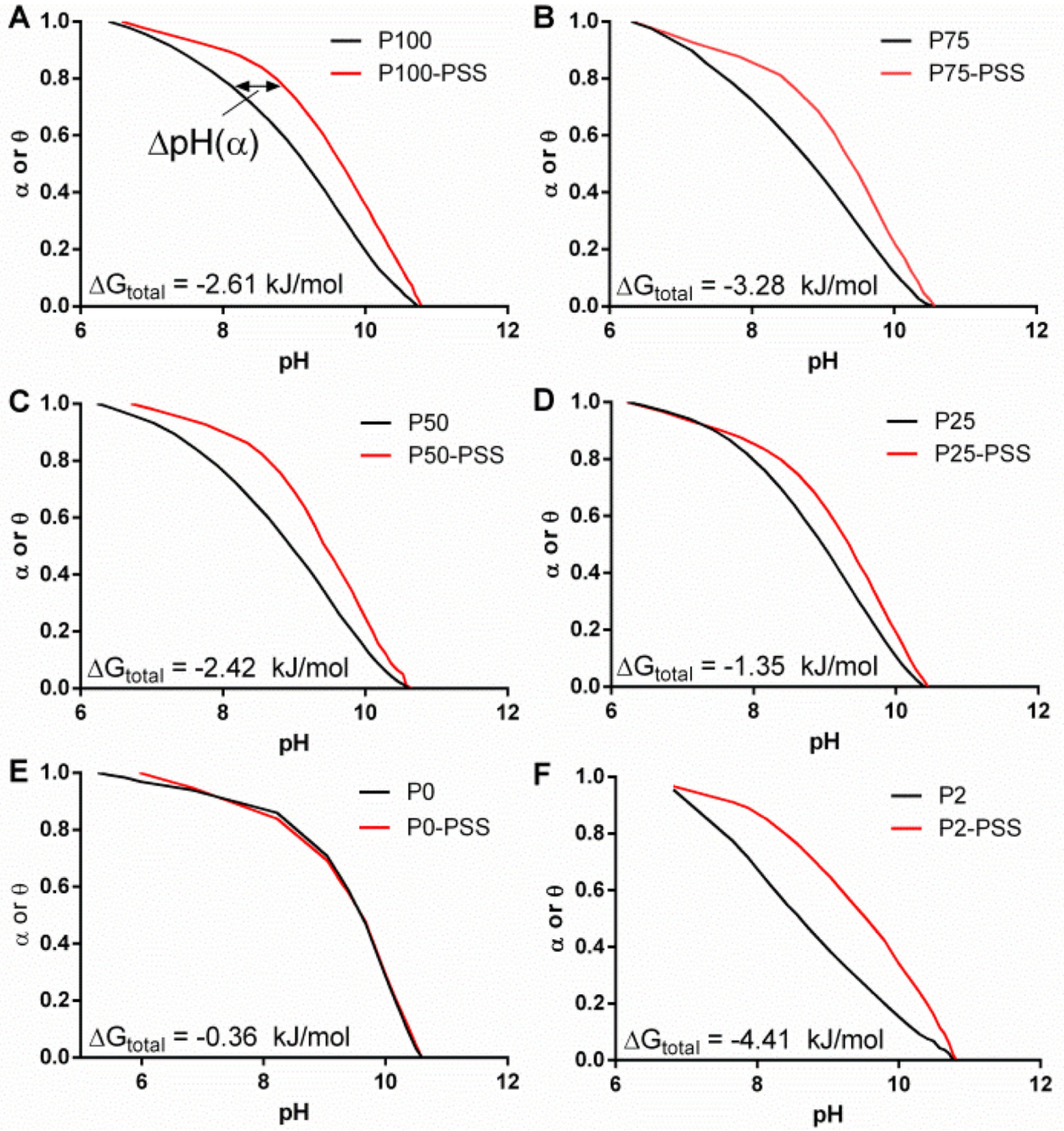

Figure 3.

α- and θ vs. pH curves for (A) **P100**, (B) **P75**, (C) **P50**, (D) **P25**, (E) **P0**, and (F) **P2** and their respective complexes with PSS

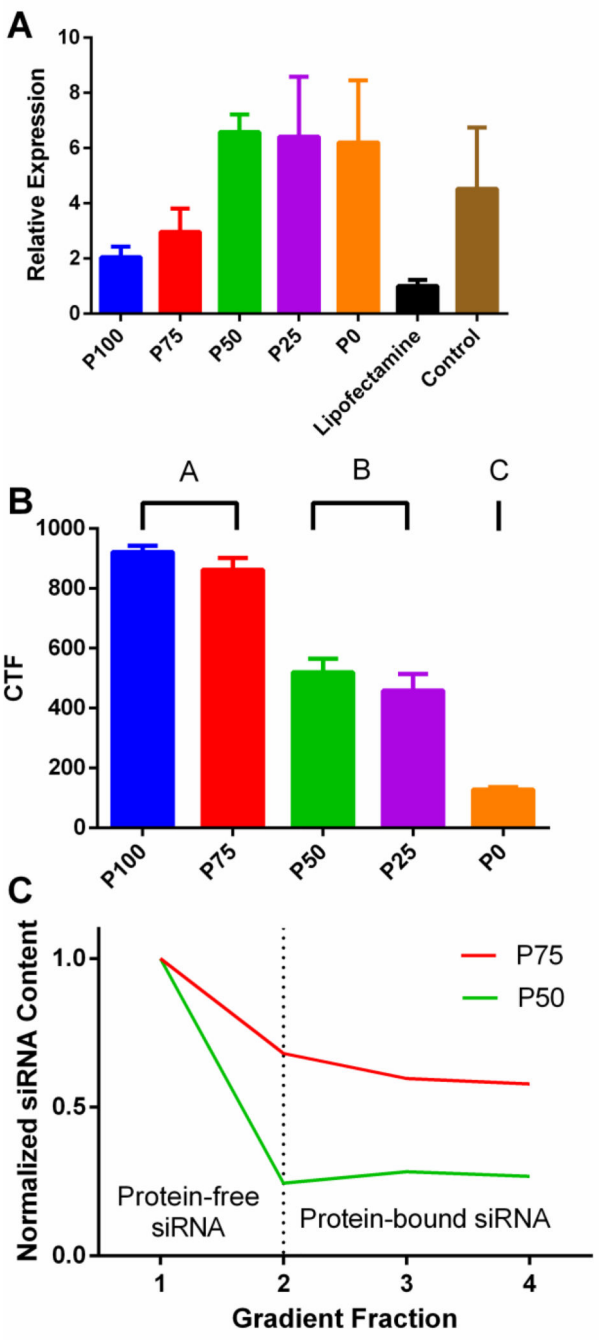

Figure 4.

(A) RT-qPCR analysis of down-regulation of human survivin mRNA by copolymer-siRNA complexes. mRNA expression normalized to Lipofectamine. (B) Corrected total fluorescence of siRNA labelled with AlexaFluor594 delivered via copolymer complexes. Samples not belonging to same letter grouping were found to have statistically significant variance via Tukey analysis. (C) Relative radio-labelled siRNA content after copolymer complex delivery and cell fractionation. Higher gradient numbers correspond to heavier fractions. siRNA content normalized to fraction 1 for each complex.

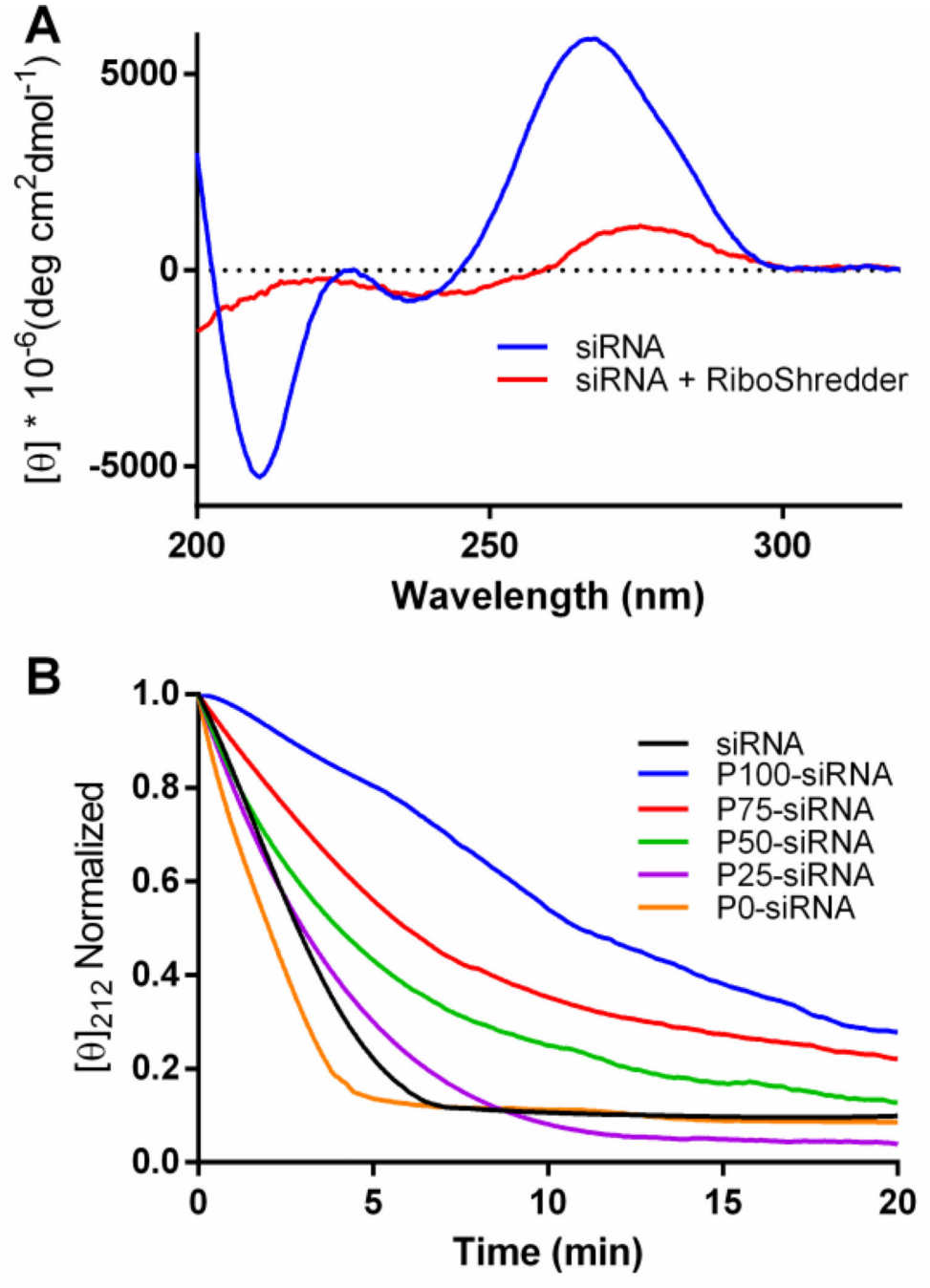

Figure 5.

(A) Molar ellipticity of siRNA before and 20 minutes after addition of Riboshredder RNase blend. (B) Enzymatic degradation of free and copolymer-complexed siRNA with Riboshredder RNase blend as monitored by the normalized disappearance of the CD band at 212 nm.

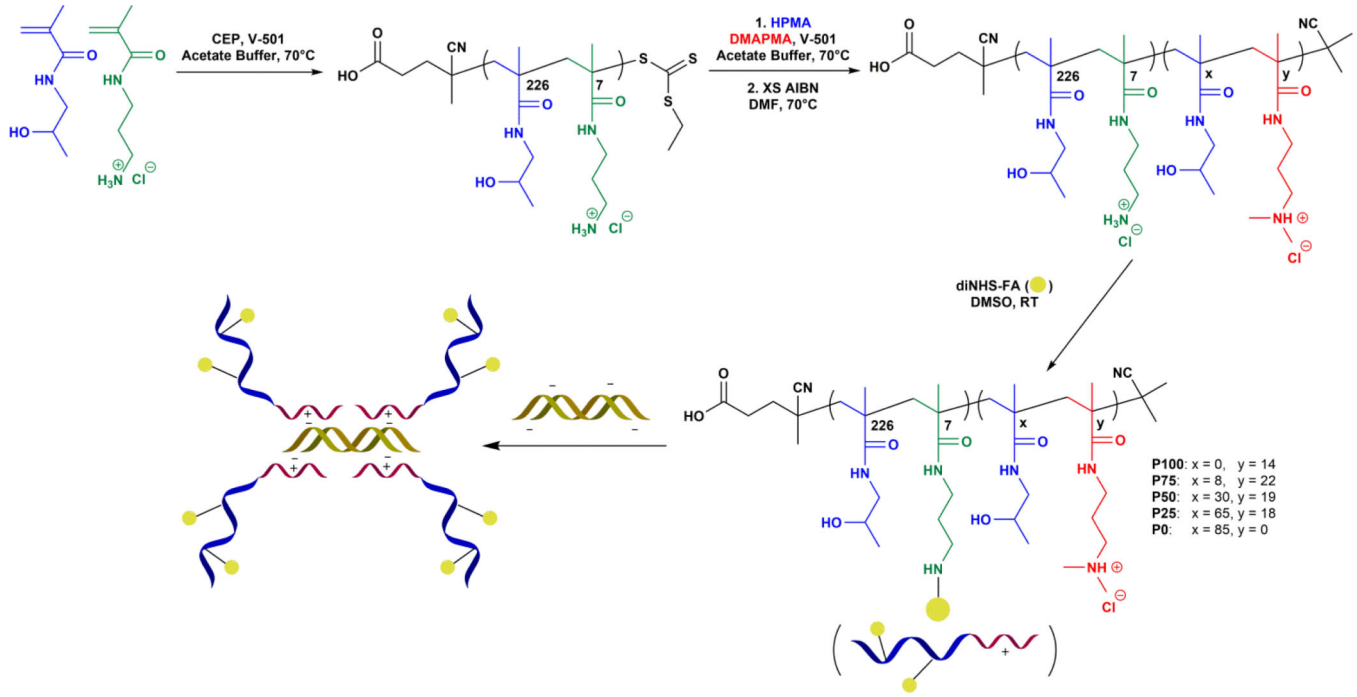

Scheme 1.

Synthetic pathway for the preparation of poly[(HPMA-*stat*-APMA)-*block*-(HPMA-*stat*-DMAPMA)] copolymers and subsequent complexation with siRNA.

Table 1

Molecular weight (number average), dispersity (Đ), composition, conversion (ρ), and dn/dc values for macroCTA and chain-extended copolymers

Sample	$M_{n,Th}$ (kDa)[a]	$M_{n,Exp}$ (kDa)[b]	Đ	Block A Comp (mol %)[c]	Block B Comp (mol %)[c]	ρ[d]	dn/dc[e]	Charge Density (%)
macroCTA	30.1	33.8	1.10	97:3	-	0.51	0.1631	-
P100	34.9	37.5	1.07	97:3	0:100	0.03	0.1616	100
P75	35.5	38.7	1.12	97:3	27:73	0.05	0.1595	73
P50	38.2	41.3	1.15	97:3	61:39	0.14	0.1607	39
P25	44.0	46.3	1.16	97:3	78:22	0.34	0.1572	22
P0	42.7	45.5	1.16	97:3	100:0	0.31	0.1614	0

[a] Theoretical M_n, ($M_{n,Th}$), calculated from conversion (ρ) using $M_{n,Th} = ([M]_o/[CTA] \times M_{w,monomer} \times \rho) + M_{w,CTA}$.

[b] Experimental M_n ($M_{n,Exp}$) was determined by aqueous SEC-MALLS.

[c] As determined by ^{1}H NMR.

[d] Conversions were determined by comparing the area of the monomeric refractive index signal at t_0 to the area at t_f..

[e] Determined by Wyatt Optilab DSP interferometric refractometer (λ = 690 nm).

Table 2

The hydrodynamic radii (R_h), ζ-potential, and percent complexed siRNA for siRNA and copolymer-siRNA complexes

Sample	R_h (nm)	ζ-potential (mV)	Complexed siRNA
P100	8.3	−1.02	75.0 %
P75	11.8	−0.44	75.9 %
P50	10.7	−1.82	79.3%
P25	7.8	−0.91	75.7 %
P0	N/A[a]	−7.55	34.7 %
siRNA	N/A[a]	−9.99	--

[a]The excess scattering compared to solvent was too low for accurate determination.